THE JOURNAL OF BIOLOGICAL CHEMISTRY
Vol. 280, No. 21, Issue of May 27, pp. 20660–20665, 2005

Printed in U.S.A.

Divergent Distribution in Vascular and Avascular Mammalian Retinae Links Neuroglobin to Cellular Respiration*

Received for publication, February 4, 2005, and in revised form, March 25, 2005
Published, JBC Papers in Press, March 25, 2005, DOI 10.1074/jbc.M501338200

Anke Bentmann‡§, Marc Schmidt‡, Stefan Reuss¶, Uwe Wolfrum‖, Thomas Hankeln, and Thorsten Burmester‡ ‡‡**

*From the ‡Department of Molecular Animal Physiology, Institute of Zoology, ¶Department of Anatomy and Cell Biology, School of Medicine, ‖Department of Experimental Morphology, Institute of Zoology, and **Institute of Molecular Genetics, Johannes Gutenberg-University of Mainz, D-55099 Mainz, Germany*

The visual function of the vertebrate retina relies on sufficient supply with oxygen. Neuroglobin is a respiratory protein thought to play an essential role in oxygen homeostasis of neuronal cells. For further understanding of its function, we compared the distribution of neuroglobin and mitochondria in both vascular and avascular mammalian retinae. In the vascular retinae of mouse and rat, oxygen is supplied by the outer choroidal, deep retinal, and inner capillaries. We show that in this type of retina, mitochondria are concentrated in the inner segments of photoreceptor cells, the outer and the inner plexiform layers, and the ganglion cell layer. These are the same regions in which oxygen consumption takes place and in which neuroglobin is present at high levels. In the avascular retina of guinea pig the deep retinal and inner capillaries are absent. Therefore, only the inner segments of the photoreceptors adjacent to choroidal capillaries display an oxidative metabolism. We demonstrate that in the retina of guinea pigs both neuroglobin and mitochondria are restricted to this layer. Our results clearly demonstrate an association of neuroglobin and mitochondria, thus supporting the hypothesis that neuroglobin is a respiratory protein that supplies oxygen to the respiratory chain.

The vertebrate retina consumes huge amounts of metabolic energy, which is used for the maintenance of the dark current of ions (1) and to replenish GTP that is converted to cGMP during phototransduction (2). The required ATP derives either form anaerobic glycolysis or from oxidative phosphorylation (3–5). Because the latter process uses molecular oxygen (O_2), it is not surprising that the retina is the highest oxygen-consuming tissue of the mammalian body (6). Lack of sufficient oxygen (hypoxia) has immediate effects on visual performance and is thought to be an important factor in a number of retinal diseases (5, 7). Oxygen is transported to the retina by blood capillaries (Fig. 1; *cf.* Ref. 5). The vascular retina of man, mouse, and most other mammals has a dual blood supply (5, 7) in which the outer retina is nourished by choroidal blood vessels that lie immediately behind the pigment epithelium. The inner retina is supplied by branches of the central retinal capillary: the deep capillary network located in the outer plexiform layer and the superficial capillaries adjacent to the ganglion cell layer. However, in species with an avascular retina, such as guinea pig or rabbit, oxygen is delivered solely by the choroidal vascular bed, whereas the deep retinal and superficial capillaries are essentially absent (8). Because oxygen diffuses just over a short distance, only the outer retina receives sufficient oxygen to sustain aerobic energy production. The inner retina of guinea pig is essentially anoxic, with oxygen partial pressures as low as 1 Torr (9).

Respiratory proteins such as myoglobin (Mb)[1] enhance the supply of the respiratory chain with oxygen (10). Neuroglobin (Ngb) is a recently identified heme-protein that resembles the Mb and hemoglobin and shares a common evolutionary origin with some invertebrate nerve-globins (11). Ngb is an intracellular protein preferentially expressed in the neurons of the central and peripheral nervous systems but also in some endocrine tissues (11–15). Like other globins, Ngb binds O_2 reversibly via an iron (Fe^{2+}) ion of the heme group with an affinity (P_{50}) of about 1 Torr, which is in the range of that of Mb (16). The precise role of Ngb in the organism is currently still not well understood. Initially, it has been suggested that Ngb carries out an Mb-like function, thus ensuring oxygen homeostasis of neurons (11). In fact, Ngb enhances the survival of cultured neuronal cells under hypoxia (17). However, the concentration of Ngb in the total brain is very low and in the range of 1 μM (11), which appears to be hardly compatible with a respiratory role of this protein. Therefore, Ngb has also been considered *e.g.* as scavenger for peroxynitrite (18) or as sensor that transmits a hypoxia signal via interaction with other proteins (19–21). Given the variety of globin functions discovered in recent years, still other roles for Ngb are conceivable, such as degradation of reactive oxygen species (ROS), NO decomposition, or a function as terminal oxidase (22–24).

In a previous study, we found that Ngb concentration in the neuronal retina of mouse is about 50–100 μM (25) and thus about 100 times higher than in total brain extracts (11). Because such concentration is in fact in the range of that of Mb in muscle cells, this observation can been taken as support for an oxygen supply function of Ngb. This hypothesis also predicts Ngb to be located in the vicinity of the mitochondria, which should be, in turn, associated with oxygen consumption rates. To further understand Ngb function, we decided to investigate

* This work was supported by grants from the Deutsche Forschungsgemeinschaft (Bu 956/5 and Ha2103/3) and the European Union (QLG3-CT-2002-01548). The costs of publication of this article were defrayed in part by the payment of page charges. This article must therefore be hereby marked "*advertisement*" in accordance with 18 U.S.C. Section 1734 solely to indicate this fact.

The nucleotide sequence(s) reported in this paper has been submitted to the GenBank™/EBI Data Bank with accession number(s) AJ781213.

§ Present address: Inst. of Immunology, University of Heidelberg, D-69120 Heidelberg, Germany.

‡‡ To whom correspondence should be addressed: Inst. of Zoology, University of Mainz, D-55099 Mainz, Germany. Tel.: 49-6131-39-24477; Fax: 49-6131-39-24652; E-mail: burmeste@uni-mainz.de.

[1] The abbreviations used are: Mb, myoglobin; Cygb, cytoglobin; Ngb, neuroglobin; PBS, phosphate-buffered saline; ROS, reactive oxygen species; RACE, rapid amplification of cDNA ends.

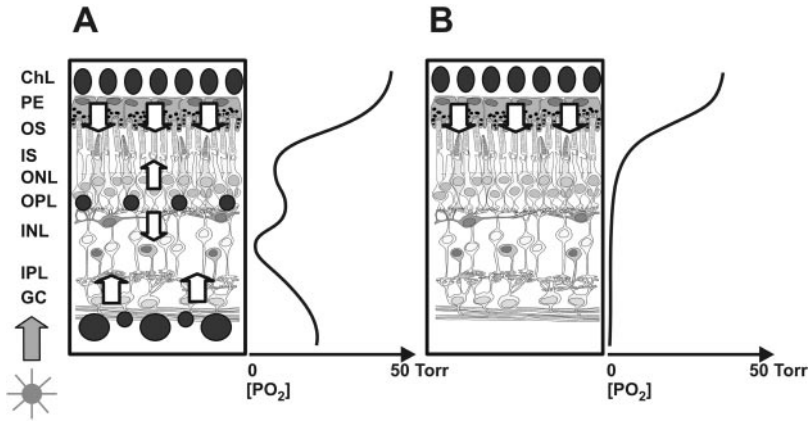

FIG. 1. **Schematic presentation of the mammalian vascular retina of rat (*A*) and avascular retina of guinea pig (*B*).** The mammalian retina is composed of well defined layers: choroidal layer (*ChL*), pigment epithelium (*PE*), outer layer of photoreceptor cells (*OS*), inner segments of photoreceptor cells (*IS*), outer nuclear layer (*ONL*), outer plexiform layer (*OPL*), inner nuclear layer (*INL*), inner plexiform layer (*IPL*), layer of ganglion cells (*GC*). The *dark circles* symbolize the capillaries, and the *open arrows* indicate the directions of oxygen diffusion. The direction of the incoming light is given at the *lower left-hand side*. At the *right side* of *A* and *B*, the oxygen profiles of rat (5, 30, 50) and guinea pig (5, 9) under normal physiological conditions are displayed.

the cellular and subcellular distribution of both mitochondria and Ngb in retinae that display different degrees of vascularization and thus oxygen supply.

EXPERIMENTAL PROCEDURES

Animals—The procedures concerning animals complied with German legislation for the protection of animals and were approved by the county government office (Bezirksregierung Rheinhessen-Pfalz). Adult pigmented BALB/c mice (*Mus musculus*) and albino rats (*Rattus norvegicus*) were maintained under constant conditions, with a 12 h:12 h light:dark regimen at room temperature (21 ± 1 °C). Food and water were supplied *ad libitum*. Guinea pigs (*Cavia porcellus*) were sacrificed immediately after purchase at the middle of the light period. For perfusion-fixation, the animals were killed with an ether overdose and transcardially perfused with 100 ml of room temperature PBS (7.5 mM Na_2HPO_4, 2.5 mM NaH_2PO_4, 145 mM NaCl), supplemented with 15,000 IU heparin/liter. Perfusion-fixation was carried out at a constant rate of 10 ml/min with 200–300 ml of ice-cold 4% paraformaldehyde, 1.37% L-lysine, 0.21% sodium periodate in PBS. The eyes were removed, postfixed for 1 h in the same fixative, and stored at 4 °C in phosphate-buffered 30% sucrose.

Cloning and Sequencing of Guinea Pig Ngb cDNA—Total RNA was extracted from guinea pig brain tissue by the guanidine hydrochloride method (26). Various degenerated oligonucleotide primers were designed according to the conserved segments of the aligned mammalian Ngb cDNA sequences. Ngb cDNA fragments were amplified by reverse transcription-PCR experiments employing the Qiagen OneStep kit according to the manufacturer's instructions. The PCR products were cloned into the pCR4-TOPO vector (Invitrogen). Sequences were obtained from both strands using a commercial sequencing service (GENterprise). The missing 3′-end of the cDNA was obtained using the RACE system of Invitrogen. The guinea pig Ngb cDNA sequence was deposited at the GenBank™/EMBL data base under the accession number AJ781213.

Antibody Preparation—Two different antigenic peptides were designed according to the conserved mammalian Ngb amino acid sequences (*cf.* Fig. 2). The first synthetic peptide covers the Ngb acid positions 47–61, with a cysteine added at the N terminus for coupling (H_2N-CRQFSSPEDCLSSPEF-$CONH_2$), the second peptide includes amino acids 55–70 (H_2N-CLSSPEFLDHIRKVML-$CONH_2$). Peptide syntheses were carried out by Eurogentec or Seqlab. The peptides were coupled to KLH and used for immunization of rabbits, employing commercial services (Eurogentec or Seqlab). The specific anti-Ngb antibodies were purified from the serum employing the synthetic peptides coupled to SulfoLink columns (Pierce) according to the instructions of the manufacturer. After elution, the antibodies were stored at 4 °C in 50 mM Tris, 100 mM glycine, pH ~7.4) supplemented with 1% bovine serum albumin and 0.05% NaN_3.

Immunohistochemistry—Indirect immunofluorescence studies on perfusion-fixed mammalian retinae were essentially performed as described previously (13, 25, 27). Briefly, the eyes were frozen in melting isopentane and 14-μm longitudinal cryosections were obtained from the retina with a Microm HM500 O microtome. The sections were mounted on Superfrost-Plus® (Roth) slides, dried, and immediately used. Nonspecific binding sites were blocked with 10% bovine serum albumin in PBS. The retina sections were incubated 2 h at room temperature with the polyclonal anti-Ngb peptide antibodies (1:5 to 1:50), polyclonal anti-von Willebrand factor antibodies (1:1,000; Abcam, Cambridge, UK), or monoclonal mouse anti-cytochrome *c* antibodies (1:200; Dianova, Hamburg, Germany), each diluted in blocking solution. The sections were washed 3 × 8 min in PBS and incubated for 90 min at room temperature in the dark with the appropriate secondary antibody (goat anti-mouse coupled to Cy2 or Cy3, or goat anti-rabbit IgG coupled to Cy3; Dianova, Hamburg, Germany), each diluted 1:200 to 1:500 in the blocking solution. The sections were washed as above and embedded in Elvanol polyvinyl alcohol (Mowiol; Calbiochem). The Hoechst dye 33258 (0.3 μg/ml) was added to the Elvanol to stain the nuclei. The sections were evaluated by a Leitz DM RD or an Olympus BX51 microscope. Photographs were taken with a digital camera. The images were combined with the Adobe Photoshop 7 program, which was also used to adjust image contrast and brightness and to add labels. Signal profiles of Ngb and cytochrome *c* from double labeling experiments were obtained and quantified employing the Scion Image program (version Beta4.02).

RESULTS

Cloning and Sequencing of Guinea Pig Ngb cDNA—A set of degenerated primers were deduced from the known mammalian Ngb coding regions and used to amplify fragments of the Ngb cDNA by reverse transcription-PCR from guinea pig total brain RNA. The 3′-end was obtained by RACE methods. However, 5′-RACE experiments failed, and the missing nucleotides of the 5′-coding region were determined by the help of degenerated primers that had been constructed according to conserved regions of rodent Ngb 5′-untranslated region. The complete Ngb coding region was eventually confirmed by reverse transcription-PCR experiments that use primers adjacent to the start and stop codons and subsequent sequencing. Like all other known mammalian Ngbs, the coding region of guinea pig cDNA covers 456 bp; 10 and 685 bp were recovered from the 5′- and 3′-untranslated regions, respectively. The deduced amino acid sequence of 151 residues displays about 90–95% amino acid identity to the other known mammalian Ngb proteins, with all key determinants required for reversible oxygen binding being conserved (Fig. 2).

Blood Capillaries in Vascular and Avascular Mammalian Retinae—The mammalian retina is built by distinct layers that are well distinguishable by light microscopy (Fig. 3*A*). We first investigated the localization and distribution of blood vessels in 14 μm thick cryo-sections of mouse (Fig. 3*B*), rat (Fig. 3*C*), and

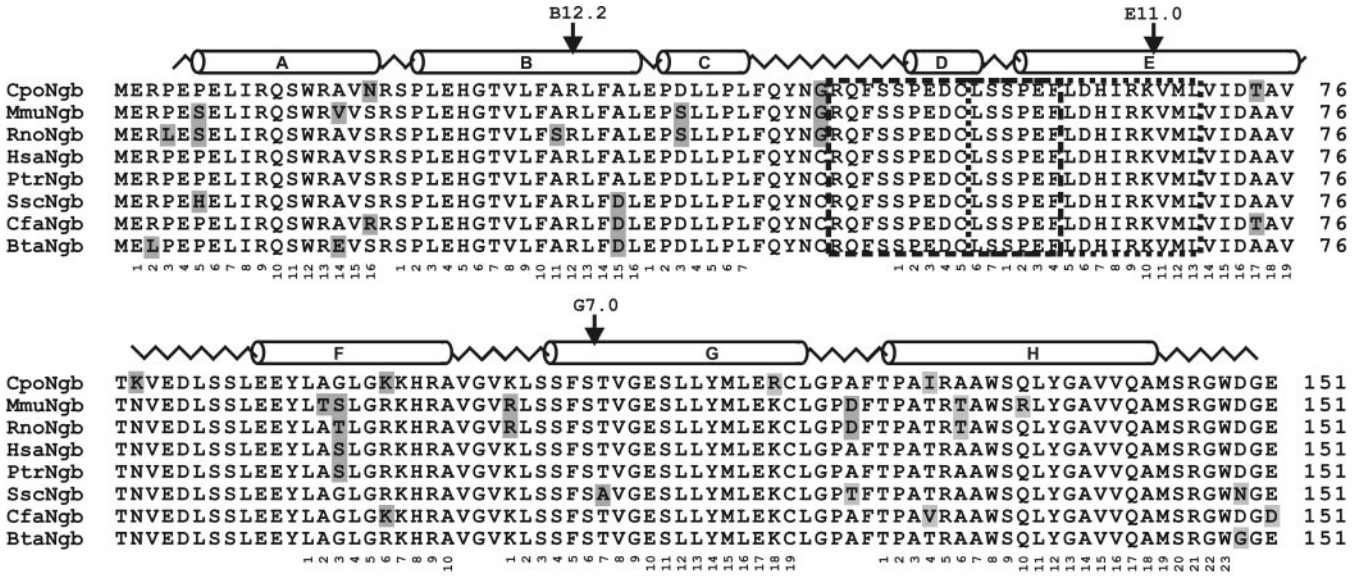

FIG. 2. **Comparison of mammalian Ngb proteins.** The deduced amino acid sequence of guinea pig Ngb (*CpoNgb*) was aligned with those of other mammals: mouse (*Mus musculus*) (*MmuNgb*), GenBank™ accession number AJ245945; rat (*Rattus norvegicus*) (*RnoNgb*), GenBank™ accession number AY066001; human (*Homo sapiens*) (*HsaNgb*), GenBank™ accession number AJ245946; chimpanzee (*Pan troglodytes*) (*PtrNgb*), GenBank™ accession number XM_522915; pig (*Sus scrofa*) (*SscNgb*), GenBank™ accession number AJ635235; dog (*Canis familiaris*) (*CfaNgb*), GenBank™ accession number AAEX01040503; cow (*Bos taurus*) (BtaNgb), GenBank™ accession number AJ635234. The globin consensus numbering is given below the alignment, and the secondary structure of human Ngb (51) is superimposed in the *upper row*. The globin α-helices are designated *A* through *H*, amino acids substitutions are *shaded*, and the intron positions in the genes are indicated by *arrows*. The *broken* and *dotted boxes* denote the two peptides used for immunization.

guinea pig (Fig. 3*D*) retinae. Using a polyclonal antibody against the von Willebrand factor, we found in the retinae of all three species strong staining of the endothelial cells of the capillaries in the choroidal layer. In mouse and rat, additional spotted signals (*arrows* in Fig. 3, *B* and C) were observed that can be attributed to the superficial capillaries in the neurofiber layer and the deep capillaries in the outer plexiform layer. This positive anti-von Willebrand factor immunostaining of the inner retina was absent in the guinea pig retina, which showed strong positive reaction only in the region of the choroidal vessels.

Ngb and Mitochondria in Vascular Retinae of Mouse and Rat—We raised two polyclonal antibodies against distinct peptides of the mammalian Ngb proteins (Fig. 2). The peptide sequences are conserved in mouse, rat, guinea pig, and other mammals. The antibodies were purified from the sera by the aid of the appropriate peptides. In immunohistochemical studies, the antibodies showed identical cytoplasmic staining on cryo-sections of mouse (Fig. 3, *E* and *F*) and rat retinae (Fig. 3*H*). In both species, positive anti-Ngb immunoreaction was found to be essentially restricted to the inner segments of the photoreceptors, the inner and outer plexiform layers, and the ganglion cells. Both nuclear layers showed only weak cytoplasmic staining. After preabsorption of the antibody with the appropriate peptide or with recombinantly expressed Ngb, the positive anti-Ngb staining disappeared (Figs. 3*G*). This demonstrated the specificity of the antibodies.

Mitochondria were identified in tissue sections employing a commercial monoclonal antibody against cytochrome *c*. Mouse and rat retinae showed identical patterns with this antibody, with a clear cytoplasmic signal (Fig. 3, *I* and *K*). Within the neuronal retina, cytochrome *c* labeling showed a punctuate pattern, consistent with the location of the immune reaction being confined to the mitochondria. Strong immunoreaction was found mainly in the inner segments of the photoreceptors, the plexiform, and the ganglion cell layers. Minor staining was also observed in endothelial cells of choroidal capillaries, as well as in the nuclear layers. Double labeling experiments employing anti-cytochrome *c* and anti-Ngb antibodies showed that the cellular localizations of Ngb and cytochrome *c* in the inner segments of the photoreceptors, the plexiform layers, and the ganglion cells are essentially identical (Fig. 3, *J* and *L*). The intensities of Ngb and cytochrome *c* signals were quantified by Scion image, which confirms their largely identical distribution. Only in the inner segments the mitochondria appeared to be evenly distributed, whereas Ngb was more concentrated in the lower sections.

Ngb and Mitochondria in the Avascular Retina of Guinea Pig—Both anti-Ngb antibodies were applied to cryo-sections of the guinea pig retina. In this species, positive anti-Ngb reaction was found to be essentially restricted to the inner segments of the photoreceptor cells (Fig. 3*M*). Strong anti-cytochrome *c* staining was observed in the inner segments, while a weak positive immunoreaction was visible in the outer segments and possibly also at some spots in the plexiform layers (Fig. 3*N*). Double staining experiments with anti-Ngb and anti-cytochrome *c* antibodies showed a largely overlapping, but slightly shifted, labeling pattern in the inner segments (Fig. 3*O*). While cytochrome *c* and thus the mitochondria are also present in the upper regions, Ngb labeling was more evenly distributed in the inner segments (Fig. 4*B*).

DISCUSSION

Oxygen Consumption and Mitochondria in the Vertebrate Retina—Since many years it has been known that the vertebrate retina consumes large amounts of oxygen and that an adequate cellular oxygen environment is crucial for the appropriate function of retinal cells (5–7). Lack of oxygen has severe effects to the visual performance (28, 29). The vertebrate retina is a highly specialized structure that is divided into morphologically and functionally distinct layers (Figs. 1 and 3*A*). This feature allows the easy correlation of measured oxygen levels with particular cellular and subcellular structures (5). In the vascular retinae of mouse and rat, oxygen partial pressures have been found to be in the range of 10–30 Torr (5, 30). It has been shown that oxygen consumption takes places mainly in

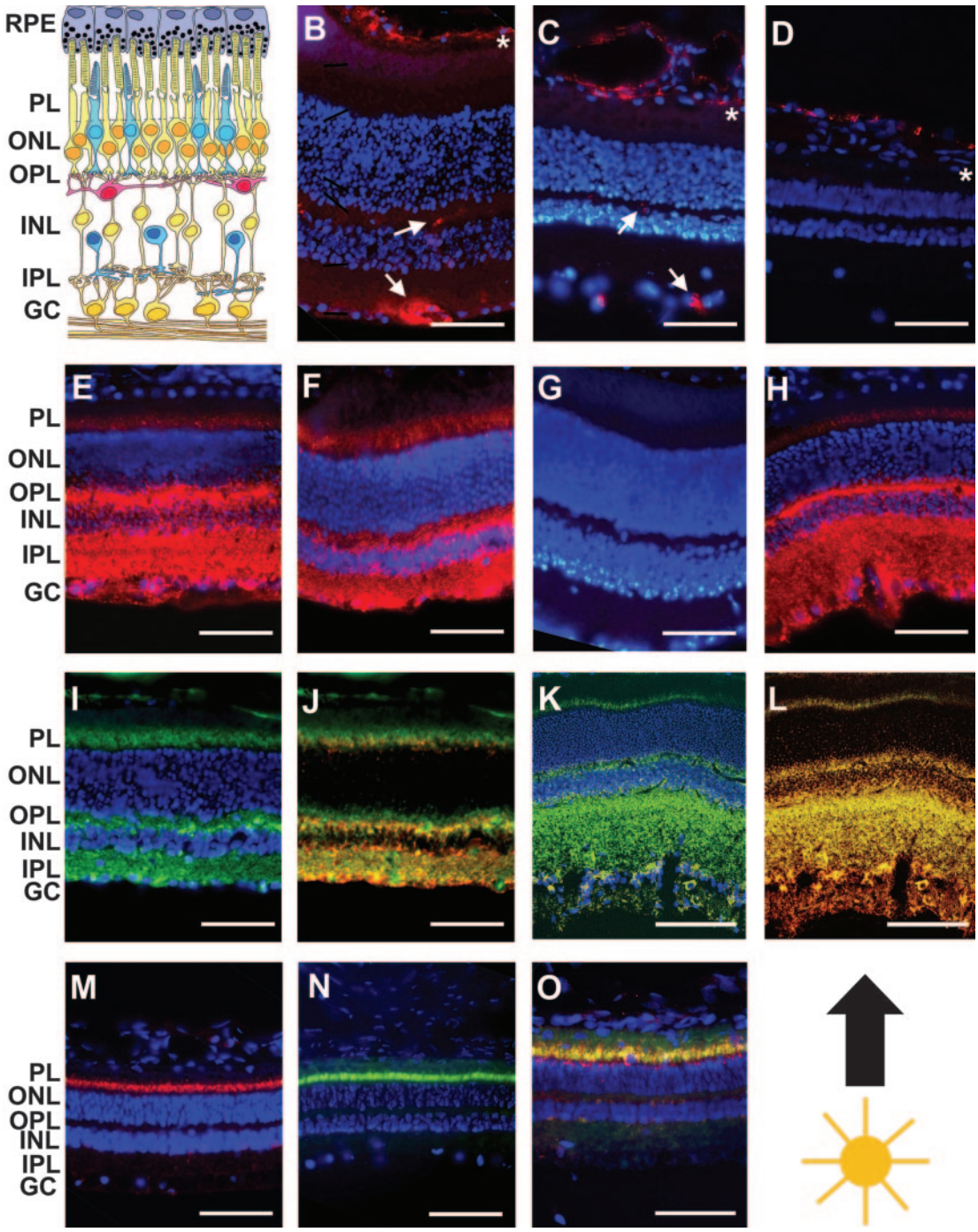

FIG. 3. **Immunohistochemical labeling of longitudinal cryosection through the retinae of mouse, rat, and guinea pig.** *A*, scheme of the vertebrate retina: retinal pigment epithelium (*RPE*) (denoted by *asterisks* in *A–C*), layer of outer and inner segments of photoreceptor cells (*PL*), outer nuclear layer (*ONL*), outer plexiform layer (*OPL*), inner nuclear layer (*INL*), inner plexiform layer (*IPL*), layer of ganglion cells (*GC*). *B–D*, endothelial cells of the blood vessels were stained with an anti-von Willebrand factor antibody (*red*). In mouse (*B*), rat (*C*), and guinea pig (*D*), the choroidal blood vessels next to the pigment epithelium (*PE*) are stained. The deep retinal and superficial capillaries visible in mouse and rat (*arrows*) are absent in guinea pig. *E–H*, localization of Ngb in mouse and rat retinae. In mouse retina, the Ngb antibodies against peptides covering amino acids 47–61 (*E*) and 55–70 (*F*) show identical staining patterns; *bright red labeling* is present in the inner segments of photoreceptors, the plexiform layers, and the ganglion cells. After preabsorption of the antibody with recombinant Ngb, the labeling disappears (*G*). The rat retina showed identical labeling as mouse retina (*H*). *I–L*, mitochondria were labeled with an anti-cytochrome *c* antibody (*green*), which stained the inner segments, the plexiform layers, and the ganglion cells in the neuronal retina of mouse (*I*) and rat (*K*). Endothelial cells were stained as well. Double labeling experiments employing anti-cytochrome *c* (*green*) and anti-Ngb (*red*) antibodies showed co-localization (*yellow*) in inner segments of the photoreceptor cells, the plexiform layers, and the ganglion cells in mouse (*J*) and rat (*K*). *M–O*, immunostaining of guinea pig retina with anti-Ngb (*M*) and anti-cytochrome *c* (*N*) antibodies. Double staining with Ngb and cytochrome *c* is shown in *O*. Co-localization is indicated by the *yellow color*. In some figures, the nuclei were blue-stained with Hoechst 33258. *Scale bars* indicate 50 μm. The *arrow* (*right side*, *bottom*) shows the direction of incoming light.

the inner segments of the photoreceptor cells, the plexiform layers, and the ganglion cells (Fig. 4*A*).

Here we have been able to associate differences in oxygen consumption rates conclusively with the distribution of mitochondria. In an aerobic metabolism, the respiratory chain in the mitochondria is the main site of oxygen consumption. Pre-

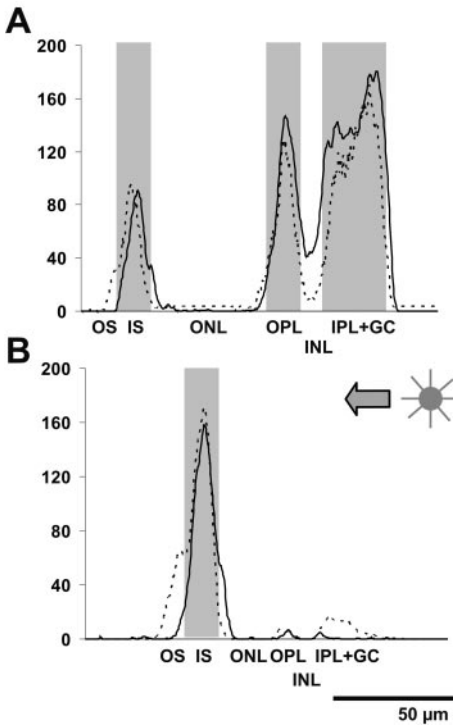

FIG. 4. **Distribution of Ngb and cytochrome *c* in the retina of mouse (*A*) and guinea pig (*B*).** The retinal layers are designated: outer layer of photoreceptor cells (*OS*), inner segments of photoreceptor cells (*IS*), outer nuclear layer (*ONL*), outer plexiform layer (*OPL*), inner nuclear layer (*INL*), inner plexiform layer (*IPL*), layer of ganglion cells (*GC*). Relative fluorescence intensity profiles were estimated from sections with a width of about 100–120 μm. The *solid lines* represent anti-Ngb fluorescence, and the *dotted lines* show anti-cytochrome *c* staining. Intensities (*y* axis) are given in arbitrary units. The *shaded regions* indicate the major oxygen consuming layers in the retina (5, 30). The *arrow* shows the incoming light; the *scale bar* indicates 50 μm.

vious studies using electron microscopic techniques, histochemical labeling, or immunohistochemical methods agreed that mitochondria are concentrated in the inner segments but were not conclusive on their distribution in the inner retina (31–34). The present study using an anti-cytochrome *c* antibody confirms an accumulation of mitochondria in the inner segments in mouse and rat retinae and shows for the first time that mitochondria are also concentrated in the plexiform and ganglion cell layers. Mitochondria appear to be essentially absent from the nuclear layers and the outer segments. The results also strongly support the calculations by Yu and Cringle (5, 30). These authors concluded from their measurements of intraretinal oxygen levels (Fig. 1) that the layers that we found in our study to contain most of the mitochondria were the main oxygen consumers of vascular mammalian retinae (Fig. 4*A*).

Ngb in Vascular Mammalian Retinae Correlates with Mitochondria Localization and Oxygen Consumption—In striated and cardiac muscles, another highly active vertebrate tissue, Mb is employed for the storage of oxygen and facilitation of oxygen diffusion (10, 35). Recently, two additional globin types have been identified in vertebrates: Ngb and cytoglobin (Cygb) (11, 36). These respiratory proteins are also present in the retinae of mouse (25), chicken (37), and fish (14), thus potentially contributing to the oxygen supply of this tissue. Because the retinal layers show distinct oxygen consumption rates (5, 30, 38, 39), it is easy to compare the distribution of Ngb and Cygb to cellular and intracellular respiration rates. In mouse, Cygb is expressed only in a subset of neurons of the brain and of the ganglion cell and inner nuclear layers of the retina (27, 40). Minor amounts of Cygb protein are also present in the inner plexiform layer, while it is absent from the outer nuclear layer and the photoreceptor cells. Thus the localization of Cygb cannot be related to mitochondria or oxygen consumption and a respiratory function of this protein is unlikely (27). In contrast to Cygb, Ngb shows enhanced expression in the murine retina (25). Its distribution in inner segments, inner and outer plexiform layers, and ganglion cells may easily be associated with the main sites of oxygen consumption. As we have shown here, Ngb distribution in mouse and rat retinae also correlates with mitochondria, which are essentially restricted to the same layers (Fig. 4). This provides an additional hint that the distribution of Ngb may in fact be correlated to oxygen consumption rates. It should be noted, however, that although the staining patterns of Ngb and mitochondria largely overlap, they are not identical. First, this observation provides evidence against a mitochondrial localization of Ngb. Second, higher cytochrome *c* levels were observed in regions that are close to capillaries and thus have higher oxygen levels. By contrast, Ngb is more concentrated in neighboring regions in which somewhat less mitochondria are present (Fig. 4) but where sufficient oxygen is still available for oxidative phosphorylation (5). Here, the respiratory protein Ngb may increase the amount of oxygen available to the mitochondria more efficiently than in regions with higher oxygen levels (see below).

Absence of Mitochondria and Ngb in the Avascular Inner Retina of Guinea Pig—By measuring intraretinal O_2 levels, Cringle and Yu (5, 9, 41, 42) concluded that the O_2 requirement of the inner retina in the guinea pig is small. While the outer retina, which is mainly composed by photoreceptor cells, accounts for more than 90% of oxygen consumption, only about 5% of the total retinal oxygen usage can be attributed to the inner retina (41). The oxygen partial pressure within the inner retina is low (1 Torr) and below the range of the assumed minimal tissue oxygen tension for mitochondrial function (26, 43). Thus the metabolism must be sustained by anaerobic mechanisms such as fermentation. The absence of mitochondria in the inner retina of guinea pigs (Figs. 3*N* and 4*B*) demonstrates that the low oxygen consumption rates are not due to a limited availability of oxygen but is a physiological characteristic of this tissue. Because of the lack of mitochondria, even an excess of available oxygen (hyperoxia) does not increase oxygen consumption rates of the inner retina of guinea pigs (9). The lack of the mitochondria in the inner retina of guinea pigs also correlates with the absence of Ngb (Figs. 3*O* and 4*B*). While the Ngb protein is probably one of the best conserved mammalian proteins (Fig. 2), we could show here that its distribution differs among species. Our observations link for the first time Ngb to oxygen consumption, even at the subcellular level.

Support for a Respiratory Function of Ngb—Intracellular globins such as the Mb are well known for their respiratory functions, supplying oxygen to the respiratory chain of the mitochondria (10, 35). However, the actual role of Ngb has remained elusive (22–24). A function of Ngb in facilitating oxygen diffusion within neurons is supported (i) by its relationship to invertebrate nerve-globins (11), for which a role as Mb-like oxygen supply protein had been established (44), (ii) by its ability to promote neuron survival under hypoxic/ischemic conditions (17), and (iii) by the enhanced Ngb concentration in the highly oxygen-consuming tissue of the retina (25). Others have considered Ngb as an oxidative stress sensor (19–21) or have suggested that Ngb is involved in the detoxification of NO or other reactive nitrogen species (18, 45). As already noted (23, 24), those functions are less likely. In particular, no correlation between Ngb and known sites of NO synthase expression in

brain or retina has been observed (12, 27). A role of Ngb in the detoxification of harmful ROS may not be formally excluded, in particular because mitochondria are known to be the main sites of ROS production (46). However, taking into account that in the retina most ROS are induced by light in the outer segments of the photoreceptor cells (47, 48) where Ngb is absent (Figs. 3 and 4), a ROS-related role of Ngb should be considered less likely.

In summary, the present study supports a respiratory function of Ngb in retinal and possibly also brain neurons. In this scenario, Ngb has a similar function as Mb (10, 35), thus facilitating the diffusion of O_2 and enhancing the flow of O_2 from the capillaries to the mitochondria. It should be noted that, like in Mb, the oxygen affinity of Ngb is higher than that of Hb but lower than that of the cytochrome oxidase (49). This positions Ngb between the hemoglobin in the capillaries and the cytochrome *c* oxidase of the respiratory chain. The oxygen partial pressures in the oxygenated, Ngb-containing regions of the retina are in the range of 10–30 Torr (5), corresponding to oxygen concentrations of 14 to 42 μM at 37 °C. Ngb concentration in the total murine retina was determined to be in the range of 50 to 100 μM (24). Because Ngb is largely restricted to the oxygen-consuming areas, local cellular and subcellular concentrations may be much higher. Thus the concentration of Ngb probably largely exceeds the free oxygen concentrations, and thus Ngb may contribute significantly to the flow of oxygen to the mitochondria. This hypothesis agrees with the observed co-localization of Ngb and mitochondria and with its absence in the anaerobic inner retina of guinea pigs. However, alternative functions of Ngb that would support the aerobic ATP production in the mitochondria by a yet unknown mechanism are still conceivable and should be addressed in future studies.

Acknowledgments—The excellent technical assistance of U. Disque-Kaiser and K. Lotz is gratefully acknowledged. We thank J. Harf for the schematic drawing of the retina. A. B., M. S., and T. B. thank J. Markl for excellent working facilities.

REFERENCES

1. Tsacopoulos, M., Poitry-Yamate, C. L., MacLeish, P. R., and Poitry, S. (1998) *Prog. Retin. Eye Res.* **17,** 429–442
2. Hsu, S. C., and Molday, R. S. (1994) *J. Biol. Chem.* **269,** 17954–17959
3. Anderson, B., and Saltzman, H. A. (1964) *Arch. Ophthalmol.* **72,** 792–795
4. Ames, A. (1992) *Can. J. Pharmacol.* **70,** S158–S164
5. Yu, D. Y., and Cringle, S. J. (2001) *Prog. Retin. Eye Res.* **20,** 175–208
6. Anderson, B. (1968) *Trans. Am. Ophthalmol. Soc.* **66,** 423–474
7. Osborne, N. N., Casson, R. J., Wood, J. P. M., Chidlow, G., Graham, M., and Melena, J. (2004) *Prog. Retin. Eye Res.* **23,** 91–147
8. Chase, J. (1982) *Ophthalmology* **89,** 1518–1525
9. Yu, D. Y., Cringle, S. J., Alder, V. A., Su, E. N., and Yu, P. K. (1996) *Am. J. Physiol.* **270,** H965–H973
10. Wittenberg, J. B., and Wittenberg, B. A. (2003) *J. Exp. Biol.* **206,** 2011–2020
11. Burmester, T., Weich, B., Reinhardt, S., and Hankeln, T. (2000) *Nature* **407,** 520–523
12. Reuss, S., Saaler-Reinhardt, S., Weich, B., Wystub, S., Reuss, M., Burmester, T., and Hankeln, T. (2002) *Neuroscience* **115,** 645–656
13. Wystub, S., Laufs, T., Schmidt, M., Burmester, T., Maas, U., Saaler-Reinhardt, S., Hankeln, T., and Reuss, S. (2003) *Neurosci. Lett.* **346,** 114–116
14. Fuchs, C., Heib, V., Kiger, L., Haberkamp, M., Roesner, A., Schmidt, A., Hamdane, D., Marden, M. C., Hankeln, T., and Burmester, T. (2004) *J. Biol. Chem.* **279,** 24116–24122
15. Laufs, T., Wystub, S., Reuss, S., Burmester, T., Saaler-Reinhardt, S., and Hankeln, T. (2004) *Neurosci. Lett.* **362,** 83–86
16. Dewilde, S., Kiger, L., Burmester, T., Hankeln, T., Baudin-Creuza, V., Aerts, T., Marden, M. C., Caubergs, R., and Moens, L. (2001) *J. Biol. Chem.* **276,** 38949–38955
17. Sun, Y., Jin, K., Mao, X. O., Zhu, Y., and Greenberg, D. A. (2001) *Proc. Natl. Acad. Sci. U. S. A.* **98,** 15306–15311
18. Herold, S., Fago, A., Weber, R. E., Dewilde, S., and Moens, L. (2004) *J. Biol. Chem.* **279,** 22841–22847
19. Wakasugi, K., Nakano, T., and Morishima, I. (2003) *J. Biol. Chem.* **278,** 36505–36512
20. Wakasugi, K., Nakano, T., and Morishima, I. (2004) *Biochemistry* **43,** 5119–5125
21. Wakasugi, K., Nakano, T., Kitatsuji, C., and Morishima, I. (2004) *Biochem. Biophys. Res. Commun.* **318,** 453–460
22. Pesce, A., Bolognesi, M., Ascenzi, P., Bocedi, A., Dewilde, S., Moens, L., Hankeln, T., and Burmester, T. (2002) *EMBO Rep.* **3,** 1146–1151
23. Burmester, T., and Hankeln, T. (2004) *News Phys. Sci.* **19,** 110–113
24. Hankeln, T., Ebner, B., Fuchs, C. Gerlach, F., Haberkamp, M., Laufs, T., Roesner, A., Schmidt, M., Weich, B., Wystub, S., Saaler-Reinhardt, S., Reuss, S., Bolognesi, M., De Sanctis, D., Marden, M. C., Kiger, L., Dewilde, S., Moens, L., Nevo, E., Avivi, A., Weber, R. E., Fago, A., and Burmester, T. (2005) *J. Inorg. Biochem.* **99,** 110–119
25. Schmidt, M., Giessl, A., Laufs, T., Hankeln, T., Wolfrum, U., and Burmester, T. (2003) *J. Biol. Chem.* **278,** 1932–1935
26. Chirgwin, J. M., Przbyla, A. E., MacDonald, R. J., and Rutter, W. J. (1979) *Biochemistry* **18,** 5294–5299
27. Schmidt, M., Laufs, T., Reuss, S., Hankeln, T., and Burmester, T. (2005) *Neurosci. Lett.* **374,** 207–211
28. Wiedman, M., and Tabin, G. C. (1999) *Ophthalmology* **106,** 1924–1926
29. Karakucuk, S., and Mirza, G. E. (2000) *Ophthalmic Res.* **32,** 30–40
30. Yu, D. Y., and Cringle, S. J. (2002) *Comp. Biochem. Physiol. A* **132,** 47–52
31. Matschinsky, F. M. (1970) in *Biochemistry of Simple Neuronal Models* (Costa, E., and Giacobini, E., eds) Vol. 2, pp. 217–243, Raven Press, New York
32. Uga, S., and Smelser, G. K. (1973) *Invest. Ophthal. Vis. Sci.* **12,** 434–448
33. Germer, A., Biedermann, B., Wolburg, H., Schuck, J., Grosche, J., Kuhrt, H., Reichelt, W., Schousboe, A., Paasche, G., Mack, A. F., and Reichenbach, A. (1998) *J. Neurocytol.* **27,** 329–345
34. Germer, A., Schuck, J., Wolburg, H., Kuhrt, H., Mack, A. F., and Reichenbach, A. (1998) *J. Neurocytol.* **27,** 347–359
35. Merx, M. W., Flögel, U., Stumpe, T., Gödecke, A., Decking, U. K., and Schrader, J. (2002) *FASEB J.* **15,** 1077–1079
36. Burmester, T., Ebner, B., Weich, B., and Hankeln, T. (2002) *Mol. Biol. Evol.* **19,** 416–421
37. Kugelstadt, D., Haberkamp, M., Hankeln, T., and Burmester, T. (2004) *Biochem. Biophys. Res. Commun.* **325,** 719–725
38. Cringle, S. J., and Yu, D. Y. (2002) *Comp. Biochem. Physiol. A* **132,** 61–66
39. Cringle, S. J., Yu, D. Y., Yu, P. K., and Su, E. N. (2002) *Invest. Ophthalmol. Vis. Sci.* **43,** 1922–1927
40. Schmidt, M., Gerlach, F., Avivi, A., Laufs, T., Wystub, S., Simpson, J. C., Nevo, E., Saaler-Reinhardt, S., Reuss, S., Hankeln, T., and Burmester, T. (2004) *J. Biol. Chem.* **279,** 8063–8069
41. Cringle, S. J., Yu, D. Y., Alder, V., Su, E. N., and Yu, P. K. (1996) *Am. J. Physiol.* **40,** H1162–H1165
42. Cringle, S. J., Yu, D. Y., Alder, V. A., and Su, E. N. (1998) *Invest. Ophthalmol. Vis. Sci.* **40,** 2307–2313
43. Epstein, F. H. (1997) *Kidney Int.* **51,** 381–385
44. Kraus, D. W., and Colacino, J. M. (1986) *Science* **232,** 90–92
45. Mammen, P. P. A., Shelton, J. M., Goetsch, S. C., Williams, S. C., Richardson, J. A., Garry, M. G., and Garry, D. J. (2002) *J. Histochem. Cytochem.* **50,** 1591–1598
46. Harper, M. E., Bevilacqua, L., Hagopian, K., Weindruch, R., and Ramsey, J. J. (2004) *Acta Physiol. Scand.* **182,** 321–331
47. Penn, J. S., and Naash, M. I., and Anderson, R. E. (1987) *Exp. Eye Res.* **44,** 779–788
48. Organisciak, D. T., Wang, H. M., Xie, A., Reeves, D. S., and Donoso, L. A. (1989) *Prog. Clin. Biol. Res.* **314,** 493–512
49. Gnaiger, E. (2003) *Adv. Exp. Med. Biol.* **543,** 39–55
50. Yu, D. Y., Cringle, S. J., Alder, V. A., and Su, E. N. (1994) *Am. J. Physiol.* **36,** H2498–H2507
51. Pesce, A., Dewilde, S., Nardini, M., Moens, L., Ascenzi, P., Hankeln, T., Burmester, T., and Bolognesi, M. (2003) *Structure* (*Camb.*) **11,** 1087–1095